Study on adverse effects of groundwater level rising induced by land creation engineering in hilly and gully area of the Loess Plateau

DUAN Xu[1]* https://orcid.org/0000-0002-8064-9226; e-mail: duanxutim@163.com

DONG Qi[2,3] https://orcid.org/ 0000-0003-3757-6823; e-mail: 38641855@qq.com

YE Wan-jun[1] https://orcid.org/ 0000-0002-8676-1753; e-mail: 63451400@qq.com

ZHOU Jia-lin[4] https://orcid.org/0000-0002-3648-7944; e-mail: jialin.zhou@griffithuni.edu.au

OH Erwin[4] https://orcid.org/0000-0002-1254-7412; e-mail: y.oh@griffith.edu.au

* Corresponding author

1 School of Architectural and Civil Engineering, Xi'an University of Science and Technology, Xi'an, Shaanxi 710054, China

2 Shaanxi Science&Technology Holding Group Co., Ltd., Xi'an, Shaanxi 710054, China

3 State Key Laboratory for Strength and Vibration of Mechanical Structures, Xi'an Jiaotong University, Xi'an 710049, China

4 School of Engineering, Griffith University, Gold Coast 7222, Australia

Citation: Duan X, Dong Q, Ye WJ, et al. (2019) Study on adverse effects of groundwater level rising induced by land creation engineering in hilly and gully area of the Loess Plateau. Journal of Mountain Science 16(12). https://doi.org/10.1007/s11629-019-5549-x

Abstract: Land creation projects have been implemented in China to expand urban space in mountainous areas. In addition to the predictable settlement brought about by filling construction, varying degrees of land subsidence and engineering failures have a demonstrated relationship to groundwater level fluctuation induced by land creation engineering. In this work, we adopted a typical large-scale land creation project, Yan'an New City in Shaanxi province, West China, as our study area. Prior to conducting the main experiment, preliminary field investigation and groundwater level monitoring were conducted to determine the groundwater fluctuation trend induced by land creation engineering. Although a blind drainage system was implemented, the depth aspect of groundwater level changes after large-scale land creation still needed to be addressed. To study the degree of impact and the settlement mechanism induced by the rising groundwater level, we conducted a Water Immersion Test (WIT) in a typical land creation site for 107 days. The rising groundwater level was simulated by injecting water from the bottom of the filling foundation. During the WIT, the soil water content, surface subsidence, and internal settlement of soil at different depths were obtained. Surface subsidence development could be categorized into four stages during the water level increase. The second stage, which is defined as the point when the groundwater level rises to 10m, marked the critical point in the process. Furthermore, it was ascertained that the local settlement in regions that were originally composed of steep slopes is larger than that in originally flat areas. In addition, ground cracks and sinkholes in the study area were inspected;

and it was determined that they would become new channels that would accelerate water infiltration and exacerbate the settlement. Based on the results from our field investigation and testing, several suggestions are proposed for land creation projects to mitigate issues associated with construction-induced groundwater level rising.

Introduction

Many of China's cities are rapidly expanding due to the country's economic growth. However, a lack of urban land restricts the cities' development, principally in mountainous areas (Bai et al. 2014). In response, local governments have encouraged and funded a plethora of land creation projects to enable city expansion in mountainous regions. This distinctive approach is designed to create flat land in the hilly and gully area of the Loess Plateau by removing mountain tops and filling the gullies with the compacted debris (Li et al. 2014; Burns 2007). In the past decade, numerous cities, such as Yan'an, Chongqing, Shiyan, Yichang, and Lanzhou have attempted this unprecedented means of expanding urban space. In addition, several airports have been built in the mountainous terrain of Jiuzhaigou, Panzhihua, Kunming, and Hechi using this method (Zhu et al. 2015; Liu et al. 2004). Yan'an New City land creation project was launched in April 2012 and is the largest such endeavor in the Loess Plateau. The plan is to double the urban area of Yan'an, creating 78.5 km² of artificial plain. Until this project, the largest expanse of artificial land created to accommodate a new city was 10.5 km².

Undoubtedly, land creation projects can contribute to the expansion of mountainous cities. Nevertheless, by drastically transforming the original landscape, these projects have triggered a variety of engineering problems, such as uneven settlement and ground cracks (Dong et al. 2015). Efforts to model the long-term settlement of these artificial foundations have been attempted through laboratory testing (Derbyshire et al. 1994) and use of PSInSAR technology (Anders et al. 2004; Yao et al. 2015; Chen et al. 2012). Furthermore, groundwater level changes are a known hidden factor that leads to an assortment of engineering difficulties in comparatively small land creation projects, such as uneven settlement, ground cracking, and filling slope sliding in artificial sites (Li et al. 2005). However, groundwater level fluctuations, and its negative impact on local engineering following land creation construction, are still poorly understood.

The safety and environmental impacts of Yan'an New City, the largest land creation project in China, continue to be a topic of rigorous debate. On the one hand, Liu (2014) reported that the construction of Yan'an New City is under strict accordance with the standards for filling construction and the land creation project is solid, safe, and sturdy. As evidence, they site the fact that the New City has experienced numerous storms without developing severe engineering problems. Conversely, other scholars claim that the local environmental impact is underestimated, and that the construction induced groundwater level modifications are impactful (Li et al. 2014). Regarding this latter point, field testing is an effective way to get empirical data to settle this dispute. Previously, field water immersion testing has been exploited to directly obtain the spatial and temporal distribution of collapsible deformation characteristics in collapsible loess foundations (Li et al. 1993; Wang et al. 2014). Such field tests have been implemented in loess areas of China, including the Gansu and Shaanxi Provinces. While this method of water immersion testing is not common, due to its high cost and long testing times, it is recognized for its reliability and contribution to a variety of crucial construction projects on the Loess Plateau (Yao et al. 2012; Wang et al. 2014). Even so, reports on field tests in land creation sites with thick layers of filling loess are still scarce.

In this study, we employed on-site investigation and field monitoring to evaluate the hydrogeological mechanism associated with and typical behavior of construction-induced groundwater level changes. Essentially, a large-scale water immersion test (WIT) was used to analyze the settlement mechanism and degree of influence induced by rising groundwater levels. Using a test format enhancement, the WIT was applied to a large trial pit in a typical land creation site, in which injected water gradually moved upward from the pit's bottom. Soil moisture

content, surface settlement, and the filling foundation's internal settlement were measured and recorded throughout. These results, in combination with damage phenomenon observations, will expand our understanding of thick filling loess moistening deformation characteristics, and help planners and engineers further enhance the stability of land creation sites by considering the impact of the underground water environment.

1 Geological Setting and Engineering Conditions

1.1 Geological setting

Yan'an New City was selected as the study area for this work. Yan'an New City lies to the north of Yan'an, which is located in the middle stretch of the Yellow River, in a hilly and gully region of the Loess Plateau, between latitudes 35°21′~ 37°31′N and longitudes 107°41′~ 110°31′E. Yan'an exhibits a temperate, semi-humid, semi-arid climate and an annual temperature of 7.7°C ~10.6°C. The annual average precipitation is 550 mm, with a maximum monthly precipitation of 81.2 mm.

The study area is composed of a landscape that was leveled to flat land by removing the mountain tops and packing the original gullies with billions of cubic metres of loess debris. As demonstrated in Figure 1a, before land creation engineering, the Qiaoer gully, which has dozens of secondary gullies on both sides, was the main gully draining to the southeast. However, after the topography was leveled, the north to south elevation difference along the Qiaoer gully was reduced. The watersheds and interzonal regions in the study area are 1100~1260 m and 950~1080 m above sea level, respectively. Following land creation engineering, an artificial flat plain was generated (Figure 1b). The highest and lowest points are 1120 and 1070 m above sea level, respectively. The ground elevation gradually reduces from north to south. Figure 2 is a geological profile of the a-a' transect in Figure 1b, which marks the location of the thickest filling.

As illustrated in Figure 2, the strata consists of Jurassic rock overlain by Neogene and then Quaternary sediments. The porous aquifer, including Lishi loess and Malan loess, ranges from 0-180 m in thickness; and in some areas, incomplete Neogene clay exists between bedrock and porous loess, which serves as an aquiclude. Furthermore, more than 55 depression springs were observed along the middle and lower reach of Qiaoer gully (Figure 1a). The maximum flow of a single spring reaches 0.45 litre per second in the
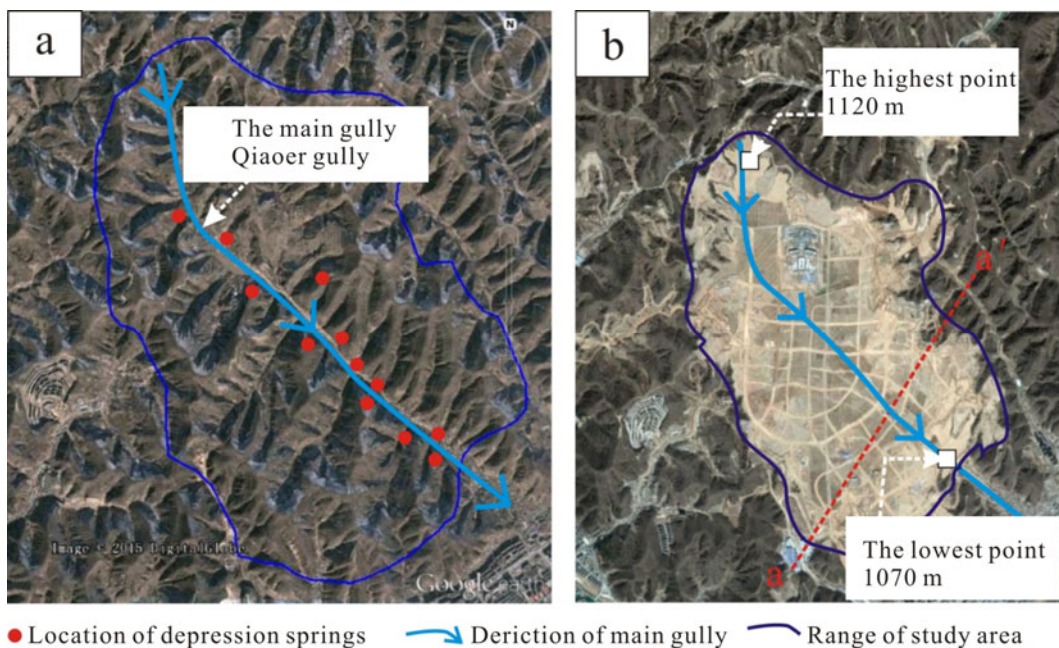

● Location of depression springs　　🠒 Deriction of main gully　　🠒 Range of study area

Figure 1 Topography in the study area: (a) before land creation engineering; (b) after land creation engineering.
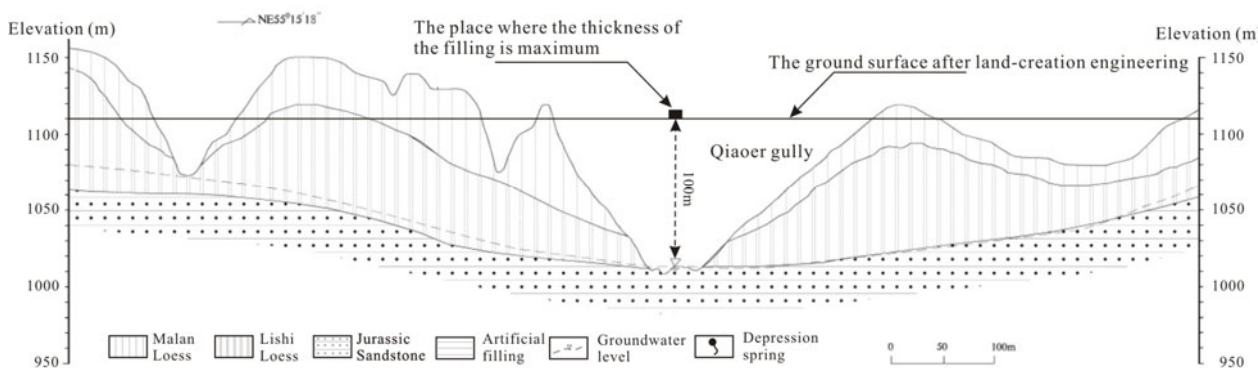
Figure 2 The geological profile of the Qiaoer gully in the study area (a-a').
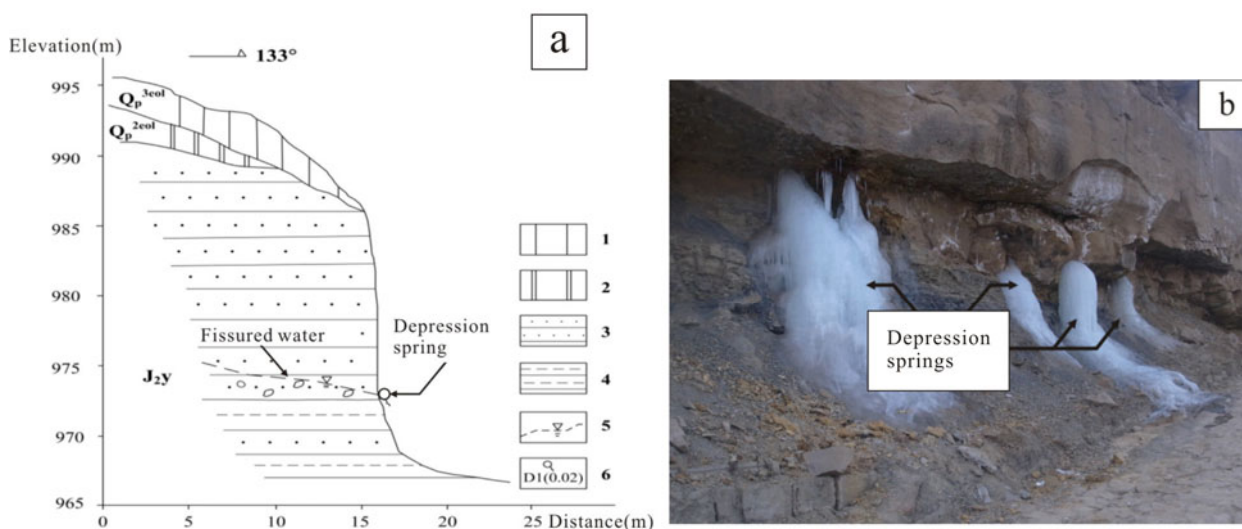

Figure 3 The typical depression spring in the study area. (a) the geological profile; (b) photograph of the depression spring.

rainy season; thus they are vital groundwater runoff channels. Figure 3 is a photograph and geological profile of a typical depression spring.

After construction, the 20-100 m thick soil filling layer became the new aquifer in the land creation area, by attaching to the original loess aquifers. Simultaneously, the original run off path was blocked, and the blind drainage systems assembled at the bottom of the gullies are anticipated to have identical effects. As shown in Figure 4, the blind drainage system envelops the whole study area, sections of which are categorized as either primary or secondary and upstream or downstream. The size of the blind drainage system (width×height) was determined based on the dimension of the gully's catchment area. Thus, the sizes of the blind drainage, at the upstream and downstream parts of the main gully, are 3.0 m×2.0 m and 5.0 m×2.0 m, respectively. The sizes of blind

drainage at the upstream and downstream of the secondary gullies are 1.2 m×1.2 m and 1.5 m×1.5 m, respectively.

1.2 Groundwater level

Although the blind drainage technique has been successfully utilized in smaller land creation projects, there is no precedent with which to determine its efficiency in a large scale land creation project. The groundwater level, under the secondary gully in the largest land creation project in China, was determined to be fairly steady after construction (Zhang et al. 2015). However, this is not indicative of the situation in the complete filled area, especially for the most concerning positions along the original main gully. Therefore, the groundwater monitoring presented in this study covers the original main gully and secondary
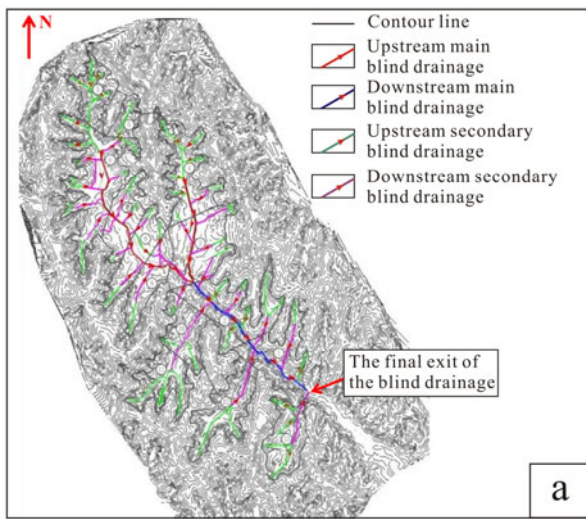
Figure 4 The blind drainage system in Yan'an New City: (a) layout of the blind drainage system; (b) the final exit of blind drainage.

gullies, such that the results comprehensively represent the entire study area.

As depicted in Figure 5, before land creation engineering, the groundwater level throughout the study area could be generally categorized into two groups. In the original gully areas, the groundwater level is between 1000 and 1040 m above sea level, and in the original watershed areas, it is > 1160 m above sea level. In this work, we used the traditional method of hydrological well observation to investigate the change of groundwater level after land creation engineering. Five groundwater monitoring points covered the original main gully and selected secondary gullies in the study area. The long term monitoring lasted 14 months with monitoring intervals of 15 days. Considering the location of the original runoff path and the filling

soil thickness, monitoring points 1, 2, 3 were arranged in the main gully from upstream to downstream, and exhibited a filling thickness of 50 m, 79 m, 100 m respectively. Monitoring points 4 and 5 were located in the secondary gullies on both sides of monitoring point 3, where the filling thickness is 35 m and 15 m, respectively.
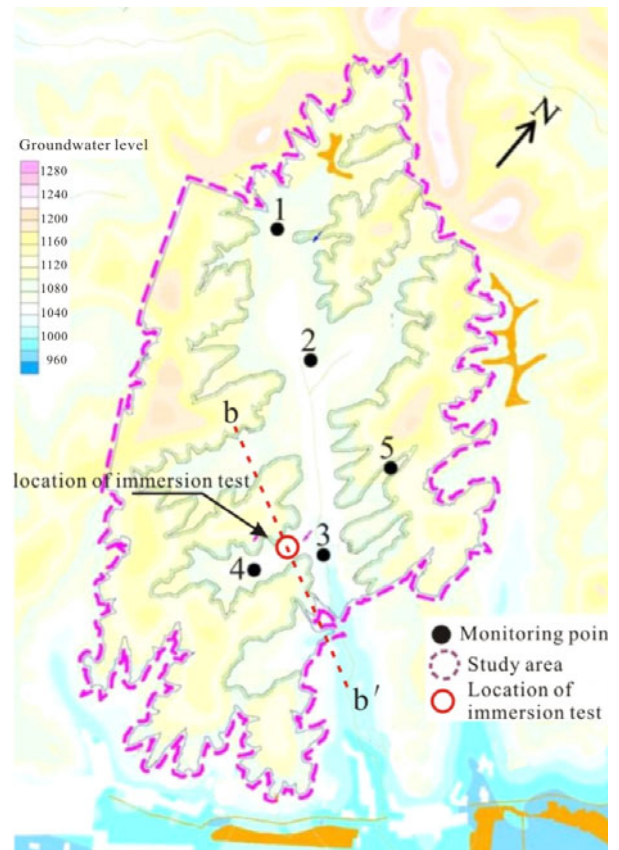

Figure 5 Distribution of groundwater before construction and layout of monitoring points.

As shown in Figure 6a, after land creation construction, the groundwater level generally rose except for the position upstream of the main gully (point 1). The groundwater level increase at the main gully's downstream location was particularly significant. Specifically, the groundwater level at monitoring point 1 fell 0.9 m during the first 6 months, then gradually swelled 0.18 m during the 6th to 14th month. These results are likely attributed to the elevation being relatively higher in the original terrain, and the blind drainage working efficiently with the aid of the terrain gradient. At monitoring point 2, the groundwater level started mounting slowly after construction, with a ratio of 2.75 cm/month. The groundwater level at
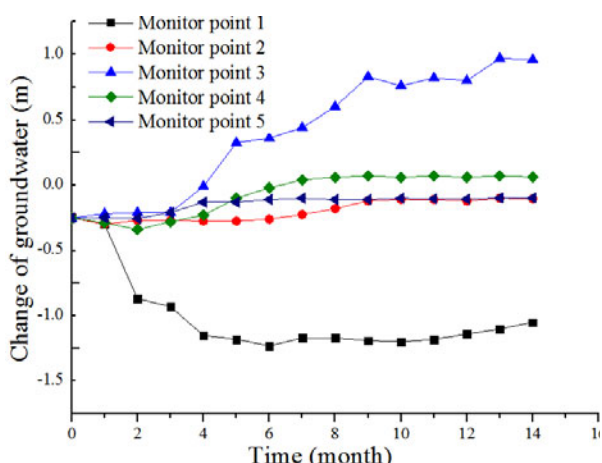
Figure 6 Change of groundwater level after land creation engineering.

monitoring point 3, which is situated downstream of the main gully, notably increased after the 4th month. The groundwater level increased in two distinct stages: 1) The groundwater level rose linearly at a rate of 26.7 cm/month for two months; 2) the rising rate gradually declined to 12.6 cm/month during the 5th to 10th months. Figure 6b shows that the extent of groundwater level rise in the original secondary gullies (points 4 & 5) is less than that along the main gully. The groundwater level of monitoring point 4 decreased 9 cm in the first two months and the rising rate reached 7.6 cm/month in the following five months. The groundwater level at point 5 rose 12 cm during the 3rd to 5th month of monitoring. The groundwater level trend from the field monitoring is comparable with the short-term prediction produced by numerical simulation (Yin et al. 2016). However, for the long-term, Yin pointed out that the groundwater level under Yan'an New City would ascend more than 30 m in 50 years after

construction. Although the growth rate presented in short-term monitoring study (14 months) was observed to decelerate, it may be manipulated by groundwater recharge periodicity and the blind drainage system efficiency. Therefore, it is critical to investigate the degree of impact and deformation mechanism in worst case scenario of construction-induced groundwater modification, within these land creation sites.

2   Test design

The groundwater level modification trend induced by land creation construction was preliminarily demonstrated based on field investigation and monitoring. Results showed that groundwater level rise is a potential threat to the underlying foundations of large-scale artificial cities. Thus, a WIT was conducted to investigate the degree of influence and the settlement mechanism induced by the rising groundwater level. The WIT testing location is marked in Figure 5. Figure 7a details the cross-sectional profile (b-b') of the testing site. As shown in Figure 7a, the test site's original terrain is typically comprised of the loess gully, and the filling's maximum thickness is ~ 35m. The test design's criteria is documented in China's code (GB50025-2004, 2004), and a test pit with a diameter and depth of 50 m and 0.8 m, respectively, was prepared to serve as the immersion zone. Additionally, 130 water injection holes, 30 cm in diameter, were drilled in the test pit and filled with gravel. The holes in the WIT design were set 4 m apart, as previous testing confirmed that a distance of 4 m between the injection holes ensures the transverse connection
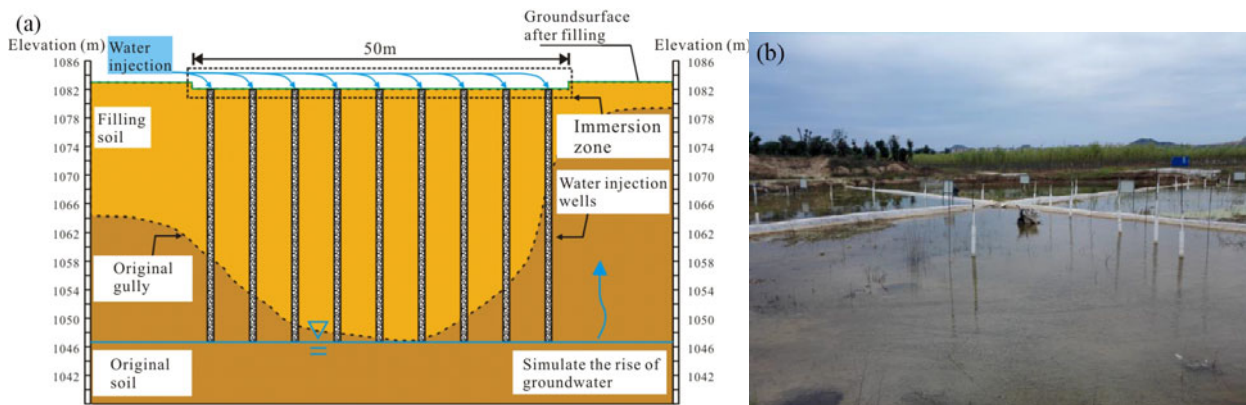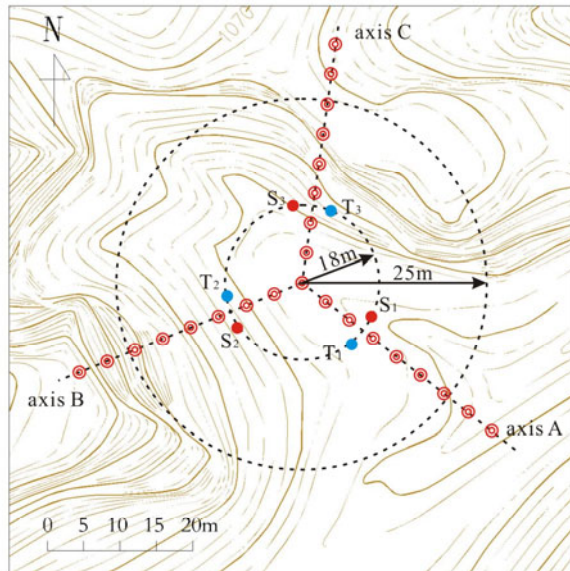

Figure 7 Design of the Water Immersion Test (WIT). (a) profile of the test site; (b) test pit with water injection.

of water. Over the test duration, ~ 5000 tons of water was injected into these water injection holes. The injected water then accumulated from bottom of the filling foundation over the course of 107 days (Figure 7b).

Figure 8 Settlement observation points and water meter layout plan in the Water Immersion Test (WIT).

In this study, we evaluated surface subsidence, soil moisture, and internal settlement. As demonstrated in Figure 8, the surface monitoring points were designed to form three axes, with a 120° angle between them. Twenty-five ground subsidence observation points (A0, A1 to A8, B1 to B8, and C1 to C8) were arranged 4 m apart on these axes. In addition, monitoring points T1, T2, and T3 were implemented to record the soil moisture throughout the experiment duration, and monitoring points S1, S2, and S3 were configured to explore the filling's internal settlement in response to the rising groundwater level. As shown in Figure 9a, b, and c, sensors for monitoring points S1, S2, S3 and T1, T2, T3 were all installed in 40 m deep exploration wells, and the slopes of the original ground in these three sections was around 10˚ (axis A), 45˚ (axis B), and 65˚ (axis C), respectively. Figure 9d illustrates the Time Domain Reflectometry (TDR) sensor and internal settlement sensor used in the WIT. Monitoring points T1, T2, and T3 consisted of 14 TDR sensors

in each exploration well, with a vertical distance of 3m between adjacent sensors. The TDR sensors are designed to record the soil moisture by using a metal probe to measure the soil's dielectric constant and convert it into volumetric water content. The monitoring points S1, S2, and S3 each consisted of 14 plates and 13 vertical displacement sensors. The plates were fixed into the inner side of the well, separated by a vertical distance of 3 m. Each plate was connected with displacement sensors, such that the change in relative displacement between the plates could replicate the filling's internal settlement.

In order to ensure the instruments were safely and accurately installed in the exploratory wells, a protective bin was designed for underground installation. As shown in Figure 10a, the protective bin's main body was made from steel with a diameter of 70 mm, and the top is connected to the rotary excavator. In addition, a specific method of underground installation was carried out. As shown in Figure 10b, the technician was secured in the protective bin, then lowered to the bottom of the exploration well via the mechanical arm of the rotary excavator. After TDR sensors were installed at the well's bottom, the protective bin gradually ascended in 3 m increments. When the protective bin reached each required location, sensors were installed at each layer. In order to prevent personnel in the well from experiencing hypoxia, oxygen was transported into the well during installation. This method was also used to install internal settlement sensors in wells S1, S2, and S3.

3 Test result and Analysis

3.1 Distribution of moisture content

The filling's moisture content at different depths reflects the movement of the injected water. During the WIT, the moisture content distribution was recorded by TDR sensors as indicated in Figure 9. The filling is thickest at T1; thus the distribution of moisture content at monitoring point T1 was selected as the typical case (Figure 11). Note that there were two flow paths of injected water in the WIT: downward seepage from the ground surface and upward seepage from bottom of the filling foundation.
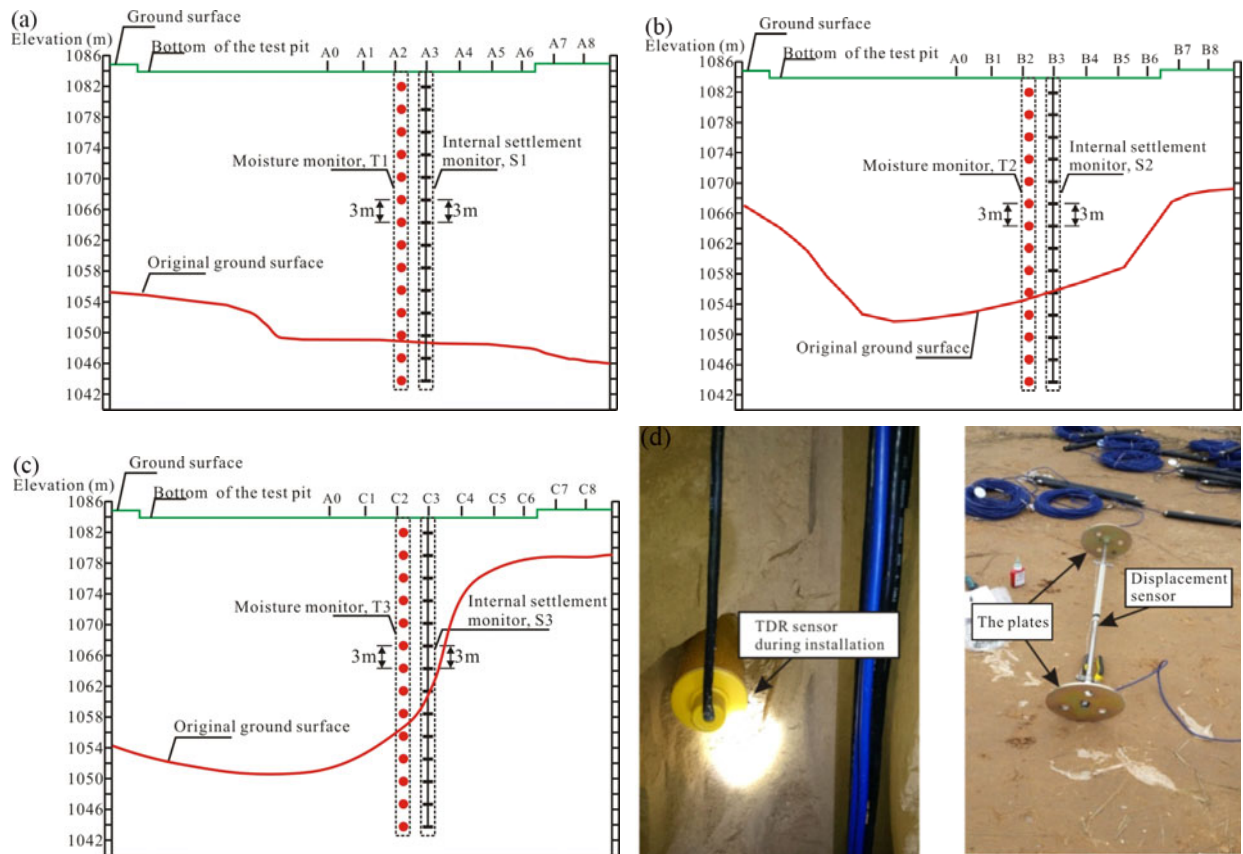
Figure 9 Cross-sectional profile of axes: (a) axis A; (b) axis B; (c) axis C; (d) the pictures of TDR sensor and internal settlement sensor.
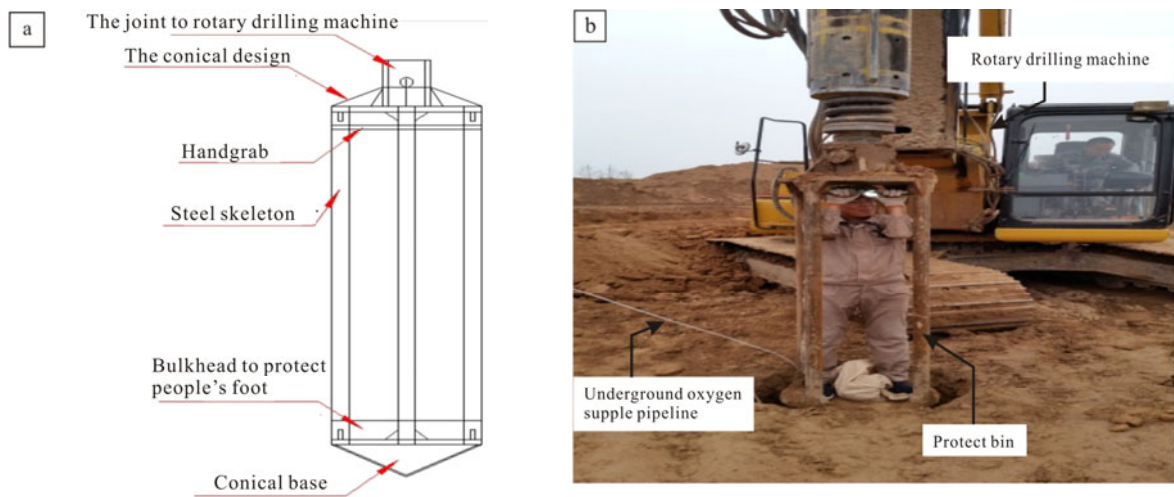

Figure 10 Installation of underground instruments: (a) design of the protect bin; (b) the process of installation.

Changes in moisture content in the 0-15 m range are controlled by seepage from the ground's surface. After water injection started, the surface soil's moisture content dramatically increased from 26% to 53.6% in the initial 15 days. Following that spike, it increased to 70%, then stabilized after 30 days. The moisture content at 5m depth increased from 22% to 28% in the initial 15 days, then swiftly rose to 49.1% over the next 15 days. The increase rate then began descending and eventually stabilized after day 30. The moisture content of soil in the 5-15 m range did not stabilize until after day 75.

Results from the lower depths, i.e., 15 m to 40 m, reflect the injected water increase. As demonstrated in Figure 11 during the initial 15 days, the moisture content at the deepest position (40 m) increased swiftly from 31.7% to 50.9% and then stabilized. Such results indicate that the injected water reached the deepest location and therefore the "artificial initial groundwater level" was successfully produced. Furthermore, the moisture content at 35 m increased from 34% to 41% over the next 15 days and also subsequently maintained stability. This implies that the groundwater level rose 5 m in the first 30 days of the WIT. Up to day 45, the moisture content at 30m was increasing. Upon reaching 47.3%, it too stabilized, suggesting that by day 45, the groundwater level had risen 10 m. Subsequently, the moisture content of the filling between 20m and 40m reached > 40% after day 75. Interestingly, the soil moisture content at 20m decreased from 44% to 40% after day 105, in response to termination of water injection. Thus, we surmise that the extent of groundwater level rise during the WIT was ~ 20m.

3.2 Characteristic of surface subsidence

Figure 12 depicts the recorded surface subsidence during the WIT. As shown in Figure12a, the surface subsidence rate does not parallel the rising artificial groundwater rate. During the initial 20 test days, the surface subsidence rate fluctuated between 0.3 mm/d and 1.6 mm/d, with an apparent peak from day 20 to 45. Furthermore, the maximum rate recorded was 7.6 mm/d. Between days 52 and 90, the secondary peak value reached 2.7 mm/d. After that, the ratio gradually dwindled to < 1.5 mm/d. Hence, the injection could be ceased according to the requirements in China's code (GB50025-2004). After terminating the water injection on day 107, the subsidence rate steadily decreased and finally stabilized at 0.45 mm/d.

As shown in Figure 12b, the surface subsidence process can be divided into three stages: A~B, B~C, and C~D. In addition, three types of settlement were identified: initiation-rapid, growth-gradual, and stability. The first stage (A~B) is characterized by the initial 32 days, during which 24% of the total subs idence occurred and the groundwater level rose 5m. The subsidence occurrence in the second stage (B~C) accounted for 73% of the total
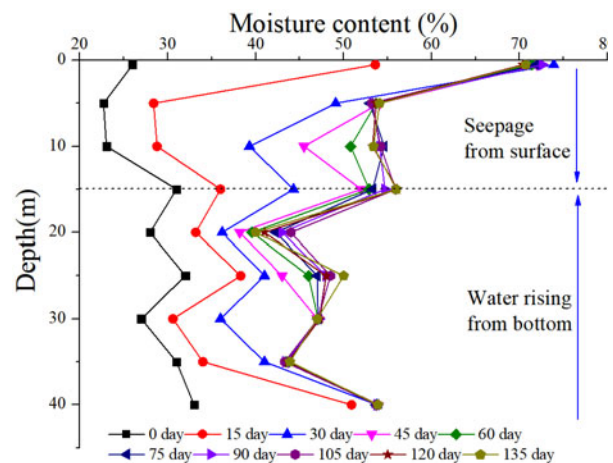

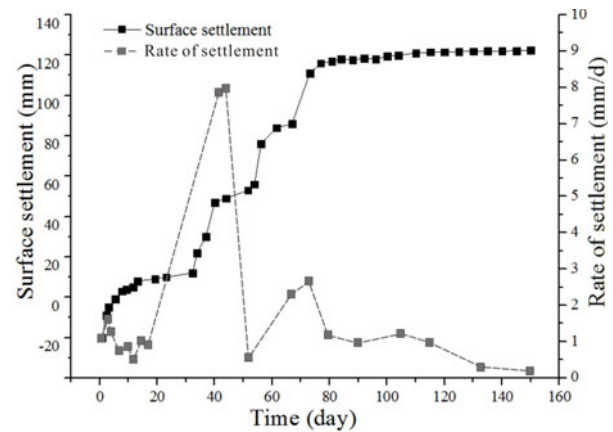Figure 11 Distribution of moisture content in Water Immersion Test (WIT).

Figure 12 Surface subsidence in the Water Immersion Test (WIT).

subsidence and the average subsidence rate reached 2.3 mm/d— identifying this as the most critical stage. In addition, the subsidence in the B~C stage is not linear, and is divided into 3 distinct parts: a~b, b~c and c~d. The type of subsidence in each part is similar to the A~B stage, but the duration is much shorter. The amount of subsidence in each part is 44mm, 30mm, and 28mm respectively, and the duration gradually decreased from 21 days to 7 days. The last stage, (C~D), lasted from day 80 to day 110. The surface subsidence was basically stable, with only 3% of the total subsidence occurring during this stage. Compared with other studies in loess area, the total subsidence in the WIT is significantly reduced from that in undisturbed loess sites (Yao et al. 2011). This phenomenon is primarily attributed to the high compaction in the filling soil; as it appears the filling's collapsibility has been basically eliminated

as anticipated. However, the moistening deformation should not be negligible given the rising groundwater level and the nonhomogeneous settlement resulting from it.

3.3 Distribution of subsidence

Typically, land creation projects are characterized with varied terrain underneath the filling foundation which is a property that should be considered when evaluating influences on the long term settlement (Dong et al. 2015; Guan et al. 2015). Figure 13a-13c depicts the surface subsidence obtained along the three axial lines (Figure 8) with respect to the original terrain.

As shown in Figure 13a, the original ground along axis A was relatively flat, with an average slope of ~ 10° and a fill thickness ranging from 30 to 35 m. From A0 to A6, the final subsidence decreased from 104 to 70 mm. The largest surface subsidence is at the test pit's central position (A0), reaching up to 104 mm. Furthermore, the subsidence from A7 to A8 (out of the test pit) decreased from 71 mm to 47 mm. This can be explained by the fact that the horizontal seepage in WIT extended to 4 m outside the test pit, and the impact attenuated from 8m to the test pit's edge. The distribution of surface subsidence along axis A is relatively uniform compared to that of axes B and C.

Figure 13b clearly demonstrates that the original ground's slope along axis B is larger than that of axis A. The average slope from A0 to B8 is ~ 35° and the local slope around B5 and B6 reaches 45°. Furthermore, in the test pit (from A0 to B6), the subsidence along axis B increased from 104 to 259 mm and the distribution of surface subsidence is not proportional to the thickness of the filling. For instance, in the original slope, the subsidence at B5 and B6 is 50% and 150% larger than that of A0; but the thickness of fill underneath B5 and B6 is 29 and 25 m, respectively, which is less than that of A0 (35m). This phenomenon is mainly due to the original slope beneath the fill, yet the reason for the conspicuous subsidence at B6 needs further study. In addition, the surface subsidence out of the test pit (B7, B8) declined from 88 mm to 75 mm, for a similar reason as described for axis A.

Figure 13c shows that the original ground's slope along axis C is larger than that of axes A and
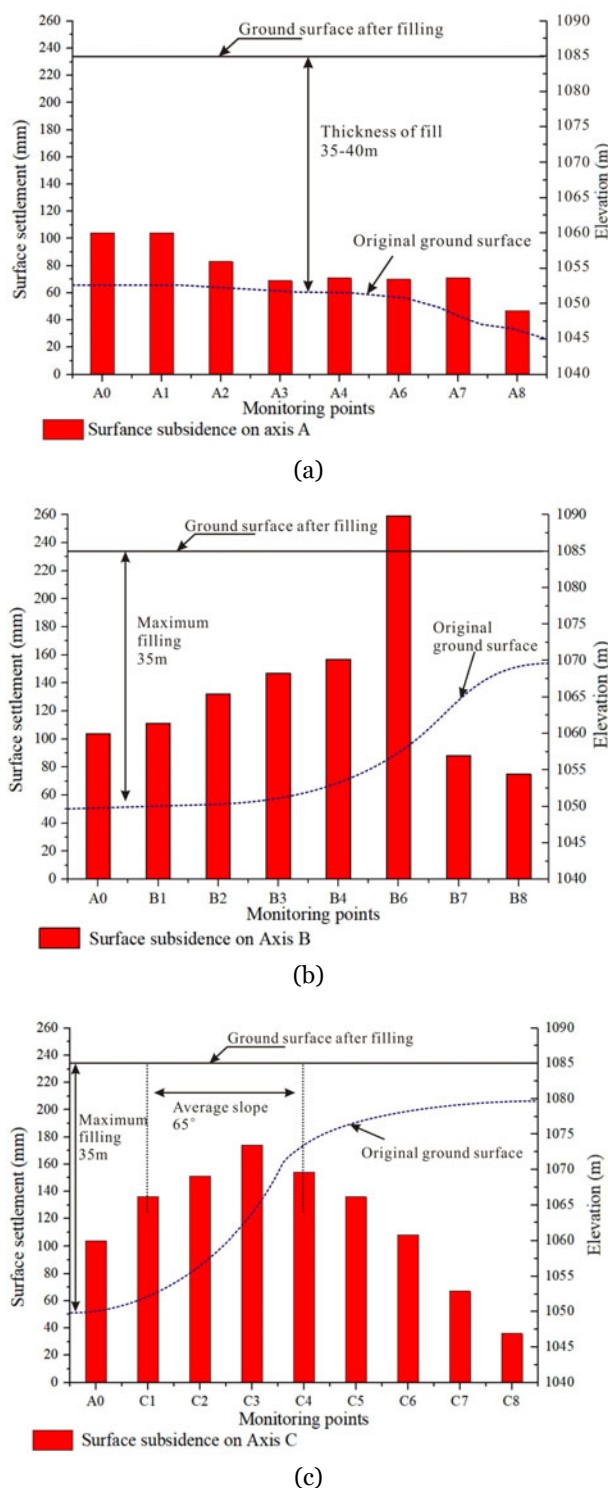

(a)

(b)

(c)

Figure 13 Distribution of surface subsidence along (a) axis A; (b) axis B; (c) axis C.

B, with an average slope of 65° from A0 to C3. In addition, like axis B, the surface subsidence from A0 to C3 increases from 104 to 174 mm, while the fill thickness decreases from 35 to 20 m.

Furthermore, from C4 to C8, the surface subsidence gradually decreases, likely because: 1) C4, C5, and C6 are located on the top platform of the original slope. The influence from the original slope gradually decreases from C4 to C6; accordingly the subsidence decreased from 154 to 108 mm; and 2) C7 and C8 are located outside the test pit. Thus, the surface subsidence declined from 67 to 36 mm, due to the reduction of seepage, paralleling the behavior of axes A and B.

Based on the results from surface subsidence monitoring during the WIT, it can be concluded that the surface subsidence in this land creation project is not uniform with the rising groundwater level due to the varied original terrain; as the surface subsidence on the original slopes is much larger than that of the original flat area.

The accumulated settlement during the groundwater level rising process, along the depth of S1, S2, and S3, is provided in Figure 14. It should be noted that 0 to 15m has been removed from the figure, since the settlement in this range was not influenced by the rising groundwater level.

As shown in Figure 14a, the internal settlement of S1 slightly increased in the initial 25 days of the WIT. The total settlement reached 3.2 mm, and the settlement below the boundary was 0.6 mm (accounting for 18%). With incessant water injection, the internal settlement generally increased but was lacking uniformity. The settlement from 16 to 25 m increased faster than the other regions. Specifically, from day 25 to day 100, local settlement in the 16 – 25 m range increased from 1.5 to 9.2 mm, and the proportion of total settlement increased from 49% to 73%. By comparison, the accumulated settlement from 25 to 35m increased from 1.3 to 2.1 mm, which accounts for 31% to 36.7% of the total settlement. Furthermore, the settlement below the boundary was 1.39 mm which comprises only 11% of the total settlement. The above results are consistent with the theoretical research on internal settlement in mountainous areas under filling projects (Zhu et al., 2015; Chen et al., 2018). To be more specific, this phenomenon is essentially impacted by the soil arch effect from original gully, which deteriorates the internal soil pressure in the middle filling, and subsequently leads to the concentrated wetting deformation above 10 m from the boundary.

Owing to the distinction of original terrain

along axes A, B and C, the distributions of internal settlement are varied. The internal settlement of S2, which is located on the original slope, is depicted in Figure 14b. Note that during the initial 25 days, the total settlement reached 7.6 mm, and the accumulated settlement below the boundary reached to 5.1 mm. These values account for 67.4% of the total settlement (both are larger than that of
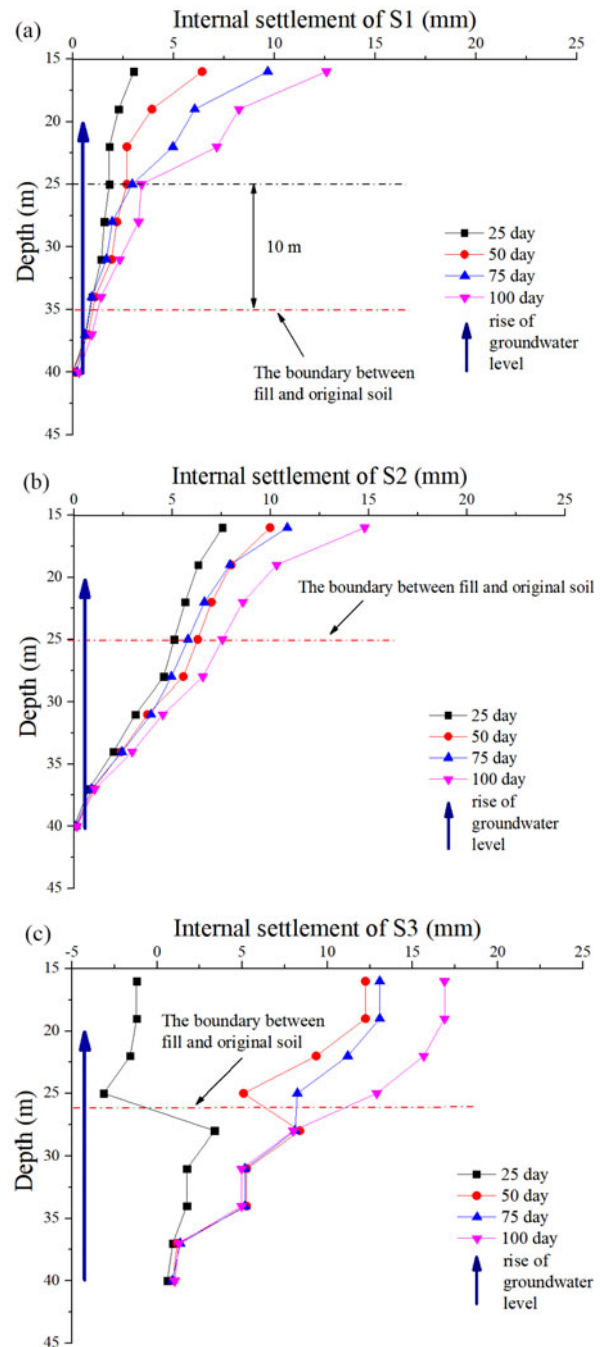

Figure 14 Distribution of internal settlement: (a) monitor point S1; (b) monitor point S2; (c) monitor point S3.

S1). Such results signify that the settlement of the original slope area (S2) is higher than that of the original flat area (S1) in the initial stage of groundwater level rise. Furthermore, from day 25 to day 100, the internal settlement of S2 generally increased, with a total settlement increase from 7.6 to 14.8 mm. Specifically, the filling soil settlement (above boundary) increased from 2.4 to 7.4 mm. Note that the increase range is larger than that of the original soil (5.2 to 7.4 mm). Up to day 100, the proportions of accumulated settlement from filling soil and original soil are both 50%.
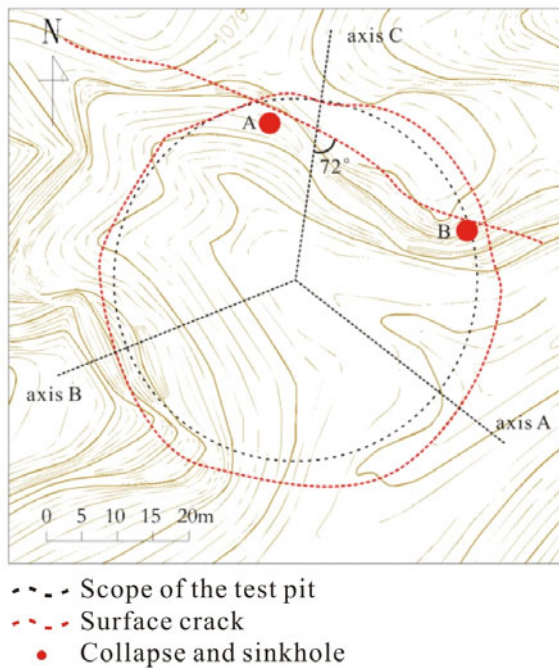

Figure 15 Crack distributions around the test pit.

The internal settlement of S3 is demonstrated in Figure 14c. During the initial 25 days, 6.6 mm of tensile deformation occurred in the range of 25 to 28 m. The deformation occurred around the boundary, and is attributed to the weak soil strength around the interface between the fill and the original slope. Slippage occurred due to either groundwater level rising or water infiltrating this location through unknown channels. Thus up to day 75, the impact of the tensile deformation can be ignored. The total settlement increased to 13.2 mm. Specifically, the filling soil settlement (above boundary) and original soil (below boundary) reached 4.8 mm (36.3%) and 8.4mm (64.7%) respectively. Up to day 100, the total settlement increased to 16.8 mm. The distribution of internal

settlement is similar to that of S2, as the accumulated settlement above the boundary reached 8.8 mm (53%). Note that the settlement increase below the boundary is less < 0.5 mm.

Based on the monitoring results discussed above, it can be concluded that internal settlement is varied due to the original terrain. For positions on original flat area with large fill thickness, the critical range of internal settlement is around 10 m above the boundary. Moreover, for the original slope area, settlement from the original soil plays an important role, especially during the initial stage of groundwater level rising. In essence, the original slope has not been given sufficient attention during construction, which resulted in two major complications: a) removal of loose soil on the original slope surface is incomplete; and b) due to the difficulty associated with hillside construction, compaction around the boundary is also inadequate. The above issues should be seriously considered in similar projects.

3.4 Phenomenon of destruction

During the WIT, a series of surface cracks emerged along the outer edge of the test pit (observed from day 20 of the WIT). Furthermore, two collapses (labeled collapse A and B) occurred in the test pit between day 30 to day 50, which was followed by the appearance of a long surface crack that continuously expanded to 75 m. As shown in Figure 15, collapses A and B, and the surface crack, were all distributed in the original steep slope area. Details of the collapses and surface crack are depicted in Figure 16. Note that the structure and size of collapse B is identical to that of collapse A. The vertical depth of collapse A was 0.8 m, and a sinkhole with 0.4 m diameter was found at the bottom. Sinkholes are recognized as resulting from mechanical erosion and dissolution of loess (Emanuele et al. 2015; Xu L et al. 2011), many geological disasters could be triggered with its impact (Bryan et al. 1997; Crosta et al. 1999). In this case, the sinkholes could become water circulation channels in the artificial filling site and further intensify the settlement. Furthermore, as shown in Figure 16b, a noticeable surface crack in the original slope area was a macroscopic phenomenon of uneven settlement. The surface crack reaches up to 70 m long and the maximum
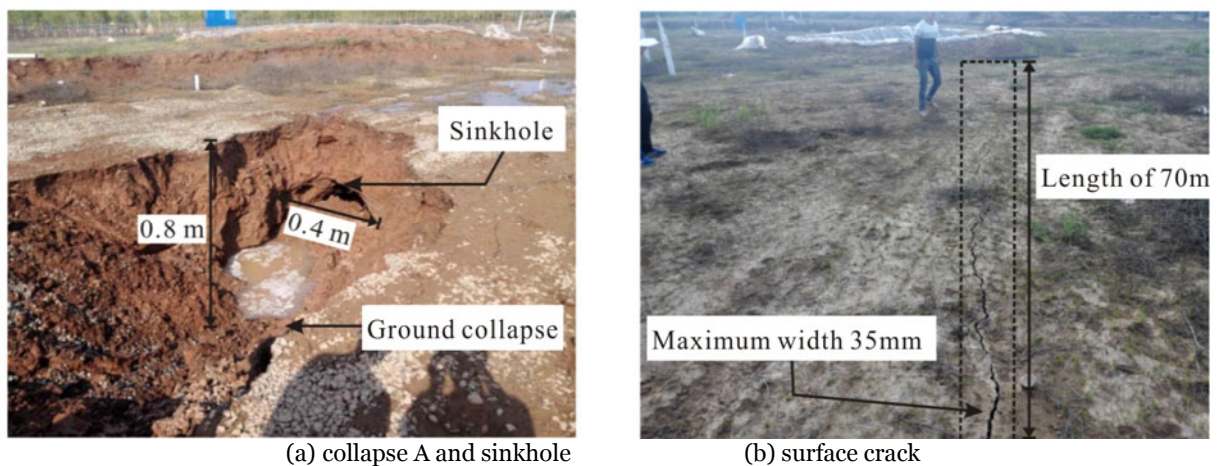
(a) collapse A and sinkhole   (b) surface crack

Figure 16 Collapse and surface crack in Water Immersion Test (WIT): a. collapse A and sinkhole; b. surface crack.

width extends to 35 mm. Thus, it is vital to assess the effects of surface cracks under the combination of infiltration and filling foundation moistening deformation. In practical projects, effective settlement monitoring is essential. Additionally, if surface cracks and sinkholes are observed, measures like ground hardening or drainage ditch control should be implemented to avoid a dangerous and costly cycle.

4 Suggestions

The engineering geology and hydrogeology problems of such enormous land creation projects are unprecedented, and the practical experience is scarce. Based on the field investigation and tests in this study, three suggestions are proposed to secure the safety of the artificial land.

1. Control and prediction of post-construction settlement should consider the influence of a changing groundwater level. Although the compactness of filling loess is strictly required in land creation projects, most standards and experience mainly come from highway subgrade filling construction. For land creation projects with filling sites that are tens of meters thick (up to 100 m), the potential wetting deformation under such high stress should not be underestimated. In the water immersion test, the filling site subsidence reached 140 mm with a groundwater level rise of 20m. The unexpected settlement will affect the safety of buildings, roads, and other structures. Furthermore, current prediction of the post-

construction settlement utilizing fixed groundwater level and soil moisture content needs to be improved based on dynamic data from a comprehensive monitoring system.

2. A comprehensive monitoring system that combines groundwater, ground settlement, and soil moisture content, needs to be established for land creation projects. In this study, the initial risk identification came from the results of field investigation and groundwater monitoring. With the design and operation of a small scale, comprehensive monitoring system, the relationship between ground settlement and groundwater level change can be simulated and analyzed, and the potential risks of land creation projects can be determined. Consequently, the optimization and application of such a system could illuminate the overall safety and risk associated with land creation projects, and provide dynamic parameters for accurate prediction of post-construction settlement.

3. The stability of the combined excavation and fill area in land creation projects should be addressed. In the water immersion test, the uneven settlement of the filling site on the original slope is evident, while ground cracks in this area are early evidence of problematic water migration and uneven settlement (Figure 16). Several ground cracks have already been found in recent field investigations of Yan'an New City. Field test results show that these cracks could become channels for water infiltration and ultimately aggravate subsidence. Consequently, immediate measures should be taken to avoid further destruction, such as fissure filling and ground hardening. The

potential risk of uneven settlement should also be considered during the construction of buildings and roads in these areas.

In summary, the hydrological and engineering geology problems of land creation projects put forward by Li (2014) have been partially verified and explored in this study. China's land creation projects seems not as risk free as reported (Liu 2014), but the problems are solvable, and the effect should be assessed based on actual monitoring or testing results. In addition to the suggestions proposed in this paper, research should continue to ensure China's land creation projects remain stable and secure.

5 Conclusion

In this study, field investigation and groundwater level monitoring were conducted to determine the hydrogeological conditions and groundwater fluctuation trend induced by land creation engineering. Furthermore, a large-scale water immersion test (WIT) was performed to explore the degree of influence and the settlement mechanism caused by rising groundwater. A unique method of installation for the underground sensors was designed for the WIT and successfully applied. Based on the field test results, we drew the following conclusions:

1. The groundwater level under Yan'an New City has been influenced by land creation construction, even though a large scale blind drainage system was established. Excluding the upstream position, during the 14 months after construction, the groundwater level under Yan'an New City generally ascended. Downstream of the original main gully, the groundwater level increased significantly, up to 1.3 m, with a maximum rising rate of 26.7 cm/month between the 2nd and 5th months. Further systematic

monitoring should also continue, even though the rising rate was decelerating towards the end of the monitoring period.

2. Although the collapsibility of filling loess has been basically eliminated, the moistening deformation is not negligible with a rising of groundwater level. In the WIT, the development of surface subsidence was divided into four stages, and the rate of surface subsidence in the second stage was most critical when the groundwater level rose above 10 m.

3. The original slope's terrain was determined to be a factor that affects surface subsidence during groundwater level rise. Generally, the surface subsidence on the original, steep slope was larger than that of the original flat area. Furthermore, the results from internal settlement monitoring demonstrate that settlement from the original soil plays a vital role in ground subsidence, alongside the groundwater level rise.

4. Destructive phenomena triggered by a rising groundwater level includes collapses, sinkholes, and surface cracks, which could become channels of water infiltration and aggravate the uneven settlement, thereby inducing a costly and dangerous cycle.

Acknowledgements

References

Bai X, Shi P, Liu Y (2014) Realizing China's Urban dream. Nature 509: 158-160. https://doi.org/10.1038/509158a

Li PY, Qian H, Wu JH (2014) Accelerate research on land creation. Nature 510(7503):29-31. https://doi.org/10.1038/510029a

Burns S S (2005) Bringing down the mountains: the impact of mountaintop removal surface coal mining on southern west

virginia communities, 1970-2004. Environmental History 14(2): 383-384. https://doi.org/10.1093/envhis/14.2.383

Zhu CH, Li N (2015) Post-construction settlement analysis of loess-high filling based on time-dependent deformation experiments. Chinese Journal of rock and Soil Mechanics 36(10):3023-3031. (In Chinese) https://doi.org/10.16285/j.rsm.2015.10.037

Liu YS, Li YH (2014) China's land creation project stands firm. Nature 511(July 23):410 https://doi.org/10.1038/511410c

Anders A, Moren L, Poul V L (2004) Evaluation of time-dependent behavior of soils. International Journal of Geomechanics 4(3):137-156. https://doi.org/10.1061/(ASCE)1532-3641(2004)4:3(137)

Yao YP, Liu L, Wang L, et al. (2015) Method of calculating creep deformation of high filled embankment. Chinese Journal of Rock and Soil Mechanics 36(S1):154-158. (In Chinese) https://doi.org/10.16285/j.rsm.2015.S1.026

Chen F, Lin H, Zhang Y, Lu Z (2012) Ground subsidence geo-hazards induced by rapid urbanization:Implications from InSAR observation and geological analysis. Natural Hazards and Earth System Sciences 12: 935-942. https://doi.org/10.5194/nhess-12-935-2012

Guan C, Yi Z, Runqiang Z, et al. (2018) Detection of land subsidence associated with land creation and rapid urbanization in the chinese loess plateau using time series insar: a case study of lanzhou new district. Remote Sensing 10(2): 270-293. https://doi.org/10.3390/rs10020270

Li PF, Liu H, Zhang ZY (2005) Discussion on the underground water problem of high basement in an airport. The Chinese Journal of Geological Hazard and Control 16(2):136-139 (In Chinese) https://doi.org/10.1360/gs050309

Yao ZH, Huang XF, Chen ZH (2012) Comprehensive soaking tests on self-weight collapse loess with heavy section in Lanzhou region. Chinese Journal of Geotechnical Engineering 34(1):65-74. (In Chinese)

Wang XL, Zhu YP, Huang XF (2014) Field Tests on Deformation Property of Self-Weight Collapsible Loess with Large Thickness. International Journal of Geomechanics 14(3):1-9. https://doi.org/10.1061/(ASCE) GM.1943-5622.0000320.

Emanuele I, Giovanni G, Massimiliano N (2015) Sinkhole monitoring and early warning: An experimental and successful GB-InSAR application. Geomorphology 241(15):304-314. https://doi.org/10.1016/j.geomorph.2015.04.018

Xu L, Dai FC, Tham LG (2011) Field testing of irrigation effects on the stability of a cliff edge in loess, North-west China. Engineering Geology 120(1):10-17. https://doi.org/10.1016/j.enggeo.2011.03.007

Bryan R, Jones A (1997) The significance of soil piping processes: inventory and prospect. Geomorphology 20: 209-218. https://doi.org/10.1016/S0169-555X(97)00024-X

Crosta G, Prisco CD (1999) On slope instability induced by seepage erosion. Canadian Geotechnical Journal 36(6): 1056-1073. https://doi.org/10.1139/t99-062

GB50025-2004 (2004) Code for building in collapsible loess area. (In Chinese)

Li D, He Y, Sui G (1993) A large area field immersion test research on loess Q2. Chinese Journal of Geotechnical Engineering 15(2): 1-11. (In Chinese)

Yin XX, Chen LW, He JD et al. (2016) Characteristics of groundwater flow after land creation engineering in the hilly and gully area of the Loess Plateau. Arabian Journal of Geoscience 2016(9):646-658. https://doi.org/10.1007/s12517-016-2672-7

Zhang JW, Yu YT, Li PF et al. (2016) Groundwater monitoring and analysis of high fill foundation in loess hilly-gully region. Journal of Xi'an University of Architecture & Technology 48(4):477-483. (In Chinese) https://doi.org/10.15986/j.1006-7930.2016.04.003